SUPPLEMENTAL DATA

Positional effects of AAN motifs in *rpoS* regulation by sRNAs and Hfq

Yi Peng[1], Toby J. Soper[1], and Sarah A. Woodson[2]*
[1]CMDB Program and [2]T. C. Jenkins Department of Biophysics, Johns Hopkins University, 3400 N. Charles St., Baltimore, MD 21218 USA

Supplemental Figure Legends:

Figure S1. Hfq binding of *rpoS301* Δ2-A18 fusions in vitro. Hfq binding to variants of *rpoS301* RNA was measured by native gel mobility shift as described in Fig. 3. (*A*) to (*E*) Δ2-366A18, Δ2-441A18, Δ2-484A18, Δ2-499A18, Δ2-519A18. Left, Hfq titration of *rpoS* resolved on native 6% polyacrylamide gels in $THEM_2$. Right, fraction of bound *rpoS* fit with partition functions. Δ2-366A18 and Δ2-441A18 formed two distinct RNP complexes corresponding to distal face interaction and a second unspecified site; Δ2-519A18 formed three RNP complexes corresponding to two specific interactions and additional nonspecific binding sites. By contrast, Δ2-441A18 formed only one distinct RNP complex corresponding to the first binding site (K_1). The smear around the R•H2 position may result from the unstable second RNP band. Similarly, Δ2-484A18 formed the first RNP complex and a faint second RNP band at high [Hfq], corresponding to the first and nonspecific binding sites, respectively. Both binding experiments were fit to a partition function assuming two unequal independent binding sites. The K_d values are summarized in Table S1. For wt rpoS301, the standard deviation among trials is <0.02 μM.

Figure S2. DsrA annealing to *rpoS301* Δ2-A18 RNAs *in vitro*. The annealing kinetics of DsrA and ^{32}P-labeled *rpoS301* RNAs was measured at 25 ˚C as described in Fig. 4. Gels were run continuously during the experiment so samples on the right traveled less far than those on the left. (*A*) to (*F*) Δ2, Δ2-366A18, Δ2-441A18, Δ2-484A18, Δ2-499A18, Δ2-519A18. Left, DsrA annealing kinetics without Hfq. Center, DsrA annealing kinetics of *rpoS* with 0.6 μM Hfq monomer. Right, fraction of bound *rpoS* fit with monophasic or biphasic rate equations. Note that with Hfq present, Δ2 formed the R•D•H ternary complex in the marker lane (2 hr) but not over the reaction time course of 60 min, indicating that the ternary complex formation is extremely slow. By contrast, all the Δ2-A18 fusions formed the ternary complex very rapidly. However, the ternary complex collapsed into binary complex faster than for wt rpoS301 (Fig. 4B), suggesting that it is less stable in the mutant RNAs. The k_{obs} values were summarized in Table S1. Reactions with no Hfq and for D2 with Hfq were fit to eq. 3; all others were fit to eq. (4).

Figure S3. Hfq binding of *rpoS301* single mutants in vitro. Binding experiments to ^{32}P-labeled rpoS301 RNA were performed as described in Fig. 3. (*A*) to (*E*) ΔA_6, $\Delta(AAN)_4$, Δ484, Δ499, and Δ519. Left, Hfq titration of *rpoS* resolved on native polyacrylamide gels. Right, fraction of bound *rpoS* fit to eq. (2). Higher molecular weight complexes were not resolved by the gel. ΔA_6 and $\Delta(AAN)_4$ bind to Hfq more tightly than Δ484, Δ499, and Δ519. Note that free ΔA_6, free Δ499, and Δ519 R•H complex migrated as two conformations. The K_d values are summarized in Table S1.

FIGURE S1

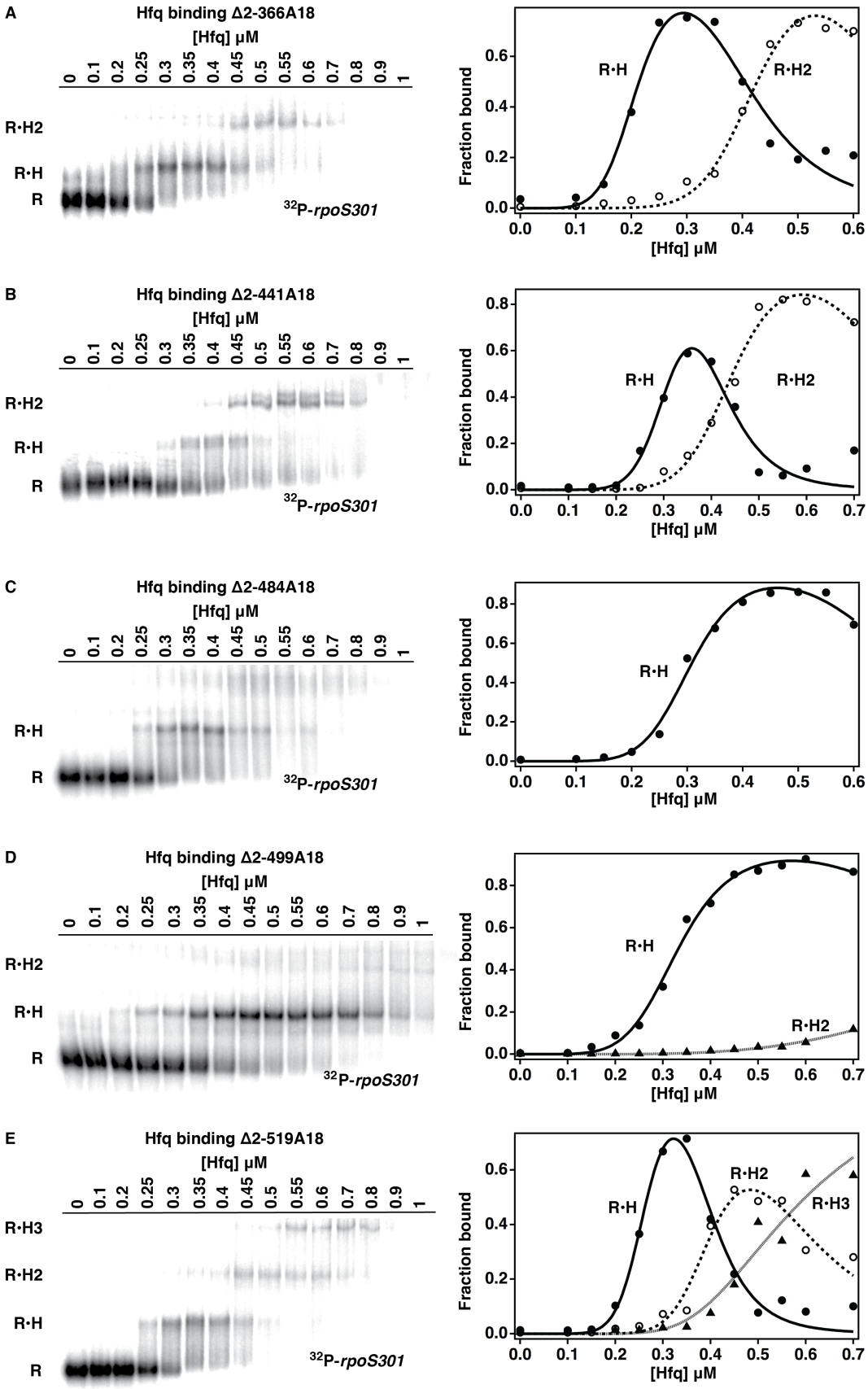
A
Hfq binding Δ2-366A18
[Hfq] μM
0 0.1 0.2 0.25 0.3 0.35 0.4 0.45 0.5 0.55 0.6 0.7 0.8 0.9 1
R·H2
R·H
R
32P-rpoS301
Fraction bound
R·H
R·H2
[Hfq] μM
B
Hfq binding Δ2-441A18
[Hfq] μM
0 0.1 0.2 0.25 0.3 0.35 0.4 0.45 0.5 0.55 0.6 0.7 0.8 0.9 1
R·H2
R·H
R
32P-rpoS301
Fraction bound
R·H
R·H2
[Hfq] μM
C
Hfq binding Δ2-484A18
[Hfq] μM
0 0.1 0.2 0.25 0.3 0.35 0.4 0.45 0.5 0.55 0.6 0.7 0.8 0.9 1
R·H
R
32P-rpoS301
Fraction bound
R·H
[Hfq] μM
D
Hfq binding Δ2-499A18
[Hfq] μM
0 0.1 0.2 0.25 0.3 0.35 0.4 0.45 0.5 0.55 0.6 0.7 0.8 0.9 1
R·H2
R·H
R
32P-rpoS301
Fraction bound
R·H
R·H2
[Hfq] μM
E
Hfq binding Δ2-519A18
[Hfq] μM
0 0.1 0.2 0.25 0.3 0.35 0.4 0.45 0.5 0.55 0.6 0.7 0.8 0.9 1
R·H3
R·H2
R·H
R
32P-rpoS301
Fraction bound
R·H
R·H2
R·H3
[Hfq] μM

FIGURE S2

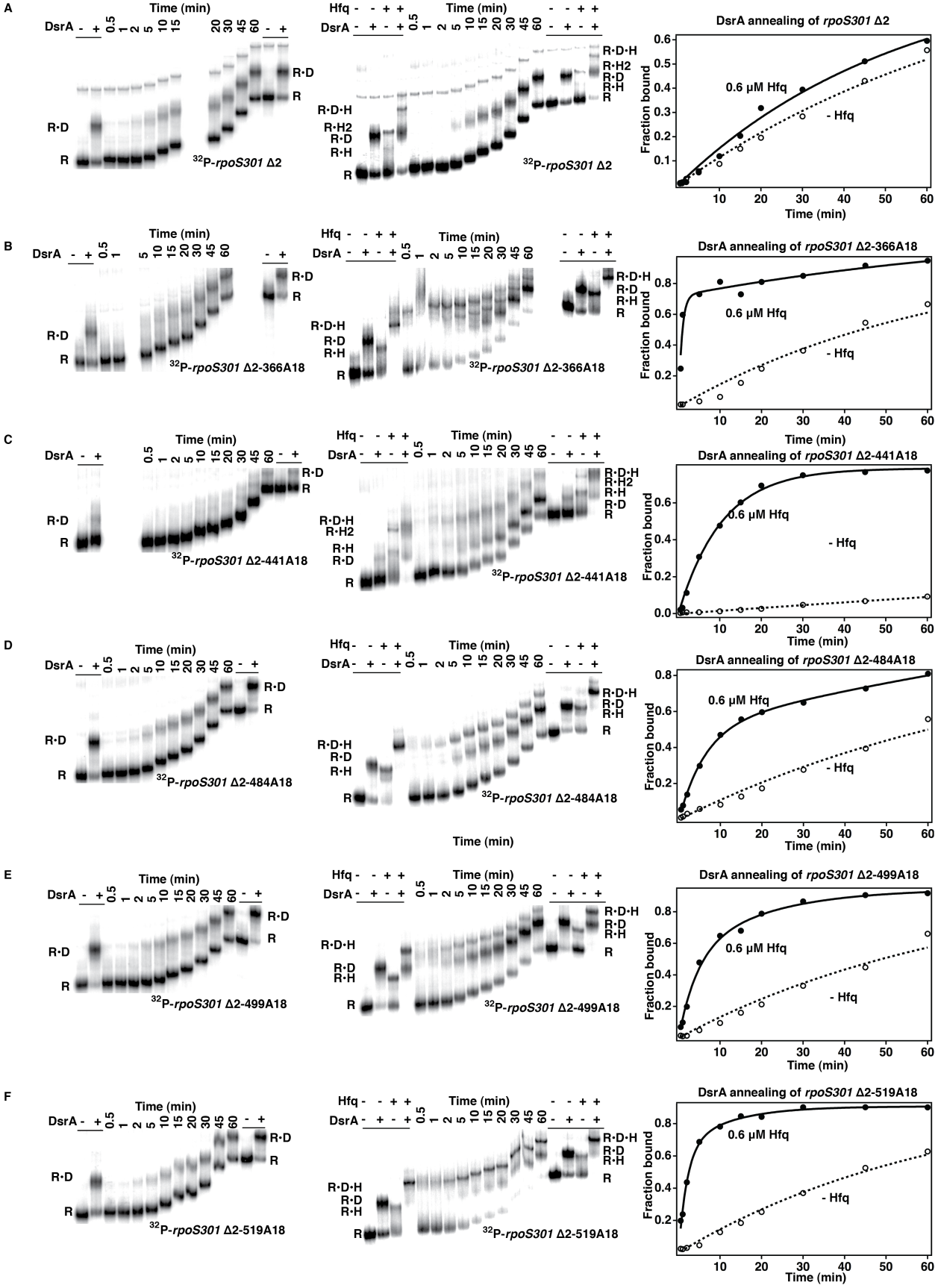
A
Time (min)
DsrA - + 0.5 1 2 5 10 15 20 30 45 60 - +
R·D
R
^{32}P-*rpoS301* Δ2
Hfq - - + +
DsrA - + - + 0.5 1 2 5 10 15 20 30 45 60 - + - +
R·D·H
R·H2
R·D
R·H
R
^{32}P-*rpoS301* Δ2
DsrA annealing of *rpoS301* Δ2
0.6 μM Hfq
- Hfq
Fraction bound
Time (min)
B
^{32}P-*rpoS301* Δ2-366A18
DsrA annealing of *rpoS301* Δ2-366A18
C
^{32}P-*rpoS301* Δ2-441A18
DsrA annealing of *rpoS301* Δ2-441A18
D
^{32}P-*rpoS301* Δ2-484A18
DsrA annealing of *rpoS301* Δ2-484A18
E
^{32}P-*rpoS301* Δ2-499A18
DsrA annealing of *rpoS301* Δ2-499A18
F
^{32}P-*rpoS301* Δ2-519A18
DsrA annealing of *rpoS301* Δ2-519A18

FIGURE S3

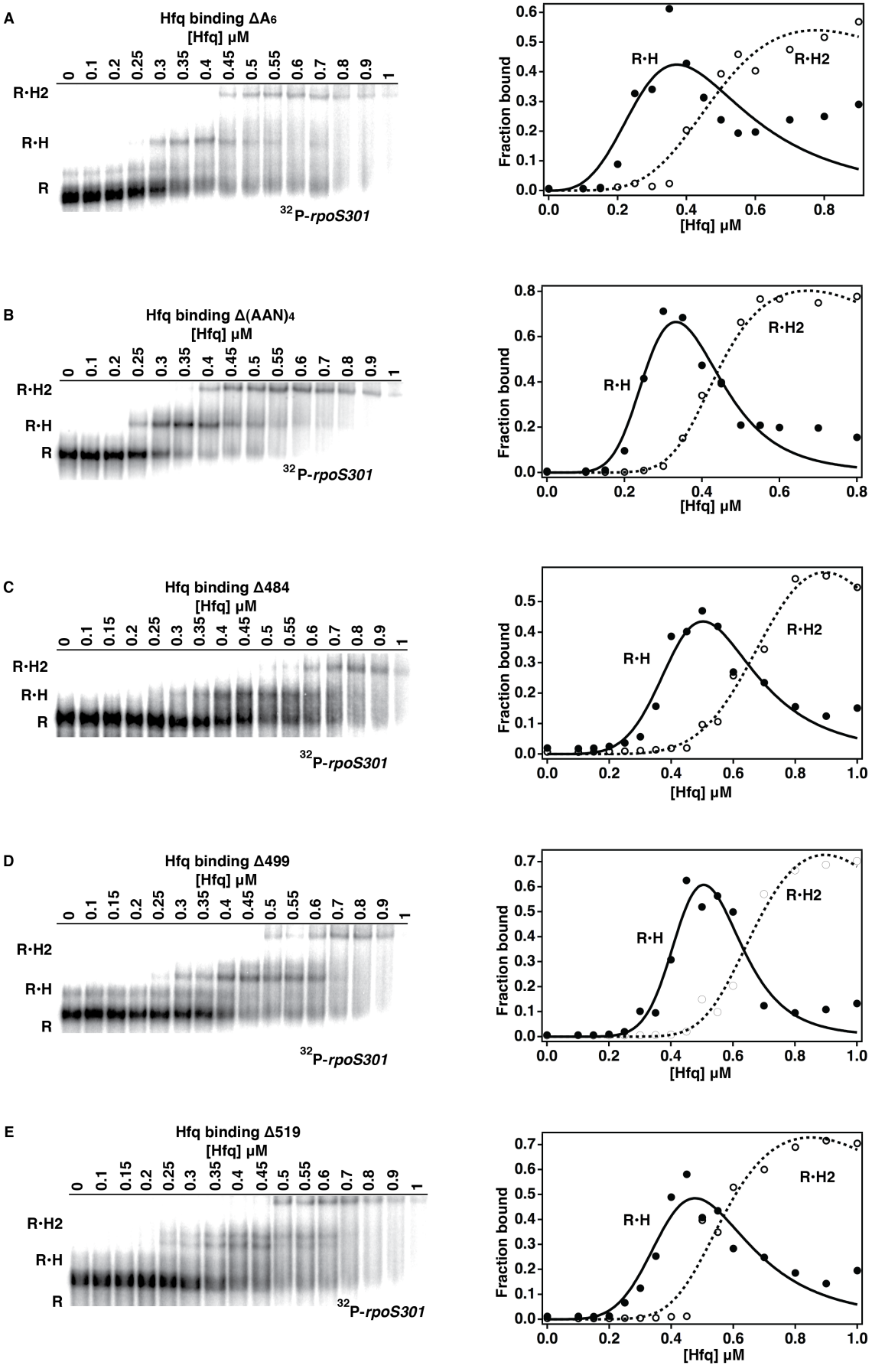
A
Hfq binding ΔA6
[Hfq] μM
0 0.1 0.2 0.25 0.3 0.35 0.4 0.45 0.5 0.55 0.6 0.7 0.8 0.9 1
R·H2
R·H
R
32P-rpoS301
Fraction bound
[Hfq] μM
B
Hfq binding Δ(AAN)4
C
Hfq binding Δ484
D
Hfq binding Δ499
E
Hfq binding Δ519

Table S1. Summary of *rpoS*•Hfq binding constants and *rpoS*•DsrA annealing rate

	Hfq binding constant K_d (μM)			DsrA annealing rate k_{obs} (min^{-1})		
rpoS301	K_1	K_2	K_{nsp}	-Hfq	+Hfq	fold of increase
wt	0.3	0.42	0.87	0.04	2.5	62.50
Δ2	-	0.4	0.74	0.012	0.018	1.50
Δ2-366A18	0.21	0.42	0.66	0.016	1.24	77.50
Δ2-441A18	0.31	0.44	0.78	0.0016	0.095	59.38
Δ2-484A18	0.31	-	0.69	0.011	0.16	14.55
Δ2-499A18	0.33	-	0.98	0.014	0.23	16.43
Δ2-519A18	0.27	0.39	0.6	0.016	0.49	30.63
ΔA6	0.33	0.43	1.04			
Δ(AAN)4	0.26	0.42	1.06			
Δ484	0.46	0.55	1.07			
Δ499	0.44	0.59	1.17			
Δ519	0.41	0.55	1.25			

The binding properties were measured by native polyacrylamide gel electrophoresis, as shown in Fig. 3 and 4, and Figs. S1, 2, and 3. The equations and calculations were described in Material and Methods.

Table S2. Primers used for mutagenesis and PCR amplification in this study

Primer name	Sequence (5' to 3', inserted or mutated sequences are highlighted)
53A18F	**AAAAAAAAAAAAAAAAAA**CGGTCACAGCGCCTGTAACGG
53A18R	GGTCGCAGTTGGCTTGTTGTTCGGC
250A18F	**AAAAAAAAAAAAAAAAAA**TGGCCGCGTTGTTTATGCTGGTAACG
250A18R	GCGGTCGCGATAATTGCCTGTCCTTTGC
366A18F	**AAAAAAAAAAAAAAAAAA**GTTAAGGCGGGGCAAAAAATAGCG
366A18R	GGACCAGCATTGTGTCGTTATGG
441A18F	**AAAAAAAAAAAAAAAAAA**TTTTGAAATTCGTTACAAGGGG
441A18R	GCAAGCGTGTTGAACTGGTTCC
484A18F	**AAAAAAAAAAAAAAAAAA**GCCGCAGCGATAAATCGGCGG
484A18R	ACGCAGCGGGTTTACGGATTTCCCC
499A18F	**AAAAAAAAAAAAAAAAAA**TCGGCGGAACCAGGCTTTTGC
499A18R	CGCTGCGGCAAATAACGCAGCGGG
519A18F	**AAAAAAAAAAAAAAAAAA**GCTTGAATGTTCCGTCAAGGG
519A18R	GCCTGGTTCCGCCGATTTATCGC
Δ484F	**CCCCC**GCCGCAGCGATAAATCGGCGG
Δ484R	ACGCAGCGGGTTTACGGATTTCCCC
Δ499F	AT**GCG**TCGGCGGAACCAGGCTTTTGC
Δ499R	CGCTGCGGCAAATAACGCAGCGGG
Δ519F	**CCCC**GCTTGAATGTTCCGTCAAGGG
Δ519R	GCCTGGTTCCGCCGATTTATCGCTGCG
Pbad-rpoS-F(1)	ACCTGACGCTTTTTATCGCAACTCTCTACTGTTTCTCCATCGGGTGAACAGAGTGCTAAC
lacZ-rpoS10aa-R(1)	TAACGCCAGGGTTTTCCCAGTCACGACGTTGTAAAACGACATCATGAACTTTCAGCGTATTCTGACTCATAAGGTGGCTCC
rpoS301F	GTGTAATACGACTCACTATAGGGTGAACGATTATCATCAAACATAATG
rpoS576R (1)	AATTCTGACTCATAAGGTGGCTCCTACC

(1) Soper, T., Mandin, P., Majdalani, N., Gottesman, S. & Woodson, S.A. 2010, "Positive regulation by small RNAs and the role of Hfq", *Proceedings of the National Academy of Sciences of the United States of America,* vol. 107, no. 21, pp. 9602-9607.

Table S3. Strains and plasmids used in this study

Strain or plasmid name	Description
PM1205(1)	MG1655 *mal*::*lacI*^{q}, ΔaraBAD, *lacI'*::PBAD-*cat-sacB*:*lacZ*, miniλtet^{R}
TSdelAdel6(2)	PM1205 *lacI'*::PBAD-*rpoS*-Δ(AAN)4ΔA6*:lacZ*
TS576(2)	PM1205 *lacI'*::PBAD-*rpoS*-Δ(AAN)4*:lacZ*
TSdel6(2)	PM1205 *lacI'*::PBAD-*rpoS*-ΔA6*:lacZ*
PY1230	PM1205 *lacI'*::PBAD-*rpoS*-Δ(AAN)4ΔA6-53A18*:lacZ*
PY1231	PM1205 *lacI'*::PBAD-*rpoS*-Δ(AAN)4ΔA6-250A18*:lacZ*
PY1203	PM1205 *lacI'*::PBAD-*rpoS*-Δ(AAN)4ΔA6-366A18*:lacZ*
PY1202	PM1205 *lacI'*::PBAD-*rpoS*-Δ(AAN)4ΔA6-441A18*:lacZ*
PY1201	PM1205 *lacI'*::PBAD-*rpoS*-Δ(AAN)4ΔA6-484A18*:lacZ*
PY1232	PM1205 *lacI'*::PBAD-*rpoS*-Δ(AAN)4ΔA6-499A18*:lacZ*
PY1233	PM1205 *lacI'*::PBAD-*rpoS*-Δ(AAN)4ΔA6-519A18*:lacZ*
PM1552(2)	TS576 *hfq::cat*
PM1556(2)	TSdelAdel6 *hfq::cat*
PY1213	PY1203 *hfq::cat*
PY1212	PY1202 *hfq::cat*

PY1211	PY1201 *hfq::cat*
PY1204	PM1205 *lacI'*::PBAD-*rpoS*-Δ484*:lacZ*
PY1237	PM1205 *lacI'*::PBAD-*rpoS*-Δ499*:lacZ*
PY1208	PM1205 *lacI'*::PBAD-*rpoS*-Δ519*:lacZ*
PY1238	PM1205 *lacI'*::PBAD-*rpoS*-499A18*:lacZ*
PY1239	PM1205 *lacI'*::PBAD-*rpoS*-519A18*:lacZ*
pRpoS576(3)	Topo based template containing full-length rpoS
pRpoSDA6(2)	Topo based template containing full-length rpoS with A6 mutation
pRpoSDAAYAA(2)	Topo based template containing full-length rpoS with (AAN)4 mutation
pRpoS-HBM(2)	Topo based template containing full-length rpoS with A6(AAN)4 mutation
pRpoS-Δ2-53A18	Topo based template containing full-length rpoS with A6(AAN)4 mutation and A18 insertion at position 53
pRpoS-Δ2-250A18	Topo based template containing full-length rpoS with A6(AAN)4 mutation and A18 insertion at position 250
pRpoS-Δ2-366A18	Topo based template containing full-length rpoS with A6(AAN)4 mutation and A18 insertion at position 366
pRpoS-Δ2-441A18	Topo based template containing full-length rpoS with A6(AAN)4 mutation and A18 insertion at position 441
pRpoS-Δ2-484A18	Topo based template containing full-length rpoS with A6(AAN)4 mutation and A18 insertion at position 484
pRpoS-Δ2-499A18	Topo based template containing full-length rpoS with A6(AAN)4 mutation and A18 insertion at position 499
pRpoS-Δ2-519A18	Topo based template containing full-length rpoS with A6(AAN)4 mutation and A18 insertion at position 519

pRpoS-Δ484	Topo based template containing full-length rpoS with U-rich motif mutation at position 484
pRpoS-Δ499	Topo based template containing full-length rpoS with A-rich motif mutation at position 499
pRpoS-Δ519	Topo based template containing full-length rpoS with U-rich motif mutation at position 519
pRpoS-wt-499A18	Topo based template containing full-length rpoS with A18 insertion at position 499
pRpoS-wt-519A18	Topo based template containing full-length rpoS with A18 insertion at position 519
pBRplac(4)	Amp^r, Plac promoter based expression vector
pDsrA(2)	AatII-EcoRI DsrA-containing fragment cloned into pBR-plac
pRprA (2)	AatII-EcoRI RprA-containing fragment cloned into pBR-plac
pArcZ (2)	AatII-EcoRI ArcZ-containing fragment cloned into pBR-plac
pUCT7DsrA-U6	pUC18 based DsrA with extended 3' U6 template with DraI linearization site

(1) Mandin, P. & Gottesman, S. 2009, "A genetic approach for finding small RNAs regulators of genes of interest identifies RybC as regulating the DpiA/DpiB two-component system", Molecular microbiology, vol. 72, no. 3, pp. 551-565.
(2) Soper, T., Mandin, P., Majdalani, N., Gottesman, S. & Woodson, S.A. 2010, "Positive regulation by small RNAs and the role of Hfq", Proceedings of the National Academy of Sciences of the United States of America, vol. 107, no. 21, pp. 9602-9607.
(3) Soper, T.J. & Woodson, S.A. 2008, "The rpoS mRNA leader recruits Hfq to facilitate annealing with DsrA sRNA", RNA (New York, N.Y.), vol. 14, no. 9, pp. 1907-1917.
(4) Guillier, M. & Gottesman, S. 2006, "Remodelling of the Escherichia coli outer membrane by two small regulatory RNAs", Molecular microbiology, vol. 59, no. 1, pp. 231-247.